Effects of different working frequencies on the joint formation in copper wire bonding

Reinhard Schemmel[a], Simon Althoff[a], Walter Sextro[a], Andreas Unger[b], Matthias Hunstig[b], and Michael Brökelmann[b]
[a]University of Paderborn, Chair of Dynamics and Mechatronics, Germany, reinhard.schemmel@upb.de
[b]Hesse GmbH, Paderborn, Germany, michael.broekelmann@hesse-mechatronics.com

Abstract

Ultrasonic wire bonding is used to connect the electrical terminals of semiconductor modules in power electronics. Multiple influencing factors in wedge/wedge bonding are known and extensively investigated. A constructively settable but rarely examined parameter is the bonding frequency. In case of bonding on challenging substrates, e.g. supple substructures, a high influence of the working frequency is observed. The choice of the working frequency is typically based on experimental investigations for a certain component or substrate and needs to be evaluated anew for new applications. A profound understanding of the influence of the working frequency is required to achieve a reliable bond process and a short process development. Here a generalized model for the numerical simulation of the bond formation with respect to the dynamics of the substructure is presented. The simulation results are compared to experiments using 300 μm copper wire at different working frequencies and geometries of the substructure.

1 Introduction

Ultrasonic wire bonding is an established technology used for decades to connect the electrodes of electrical devices like insulated-gate bipolar transistors (IGBT). Aluminum wire is preferably used in heavy wire applications because of its robust bonding behavior and low cost. The challenges due to rising electrical power demands in high power applications, such as wind turbines, electrical vehicles or solar modules can be seen in higher thermal and mechanical stress of the junctions. The limits of aluminum wire bonds can be overcome by copper wire bonds because of their significantly higher electrical and thermal conductivity and mechanical stability. By using copper wire, smaller chips can be operated with identical switching power at higher temperature leading to reduced costs and higher yield. For these reasons, a technology change from aluminum to copper is indispensable. Typical application fields of products equipped with copper wire bonds are, for instance the strongly growing markets of renewable energy and electric vehicles [1].

Because of the different material properties, the bonding parameters in copper wire bonding differ significantly from those of aluminum wire bonding. The ultrasonic power and the normal bonding forces are about 2 to 3 times higher. Also, the copper wire bonding process reacts more sensitive to parameter changes. This makes manufacturing of reliable copper bond connections challenging. Therefore many investigations to improve the reliability and robustness of the heavy copper wire bonding were carried out [2], [3].

Besides the main parameters of the bond process, such as the normal force, the bond duration and the ultrasonic power, a known but rarely investigated parameter is the bonding frequency. Harthoon found out in a "subsonic" Al-welding experiment with 30 Hz excitation frequency that the physical process of weld formation at low frequencies is the same as at ultrasonic frequencies [4]. The effect of the bonding frequency on the deformation behavior of Au-wire is carried out in [5]; it is shown, that with higher working frequencies the deformation ratio of the wire is smaller compared to lower frequencies and apart from that the bond strength is higher. In [6], the effect of the working frequency on the ultrasonic softening effect for Au-ball bonding and Al-wedge bonding is investigated. It is stated, that the strain rate has a significant effect on the deformation behavior of the material. Lower working frequencies (here: 60 kHz) lead to an initially softened wire by the slip of local dislocations. When deformation occurs, the material hardens and the vibration energy is transmitted to the interface between the wire and bond pad. At higher frequencies (here: 120 kHz) the wire is initially hardened due to the simultaneous shift of whole lattice planes and the vibration energy is directly transmitted to the interface with little deformation.

In this contribution, the influence of the working frequency on the bond strength of heavy wire copper bonding using a DCB substrate as well as using a challenging supple substrate is investigated. The choice of the frequency is typically based on experimental investigations for a certain component or substrate and needs to be evaluated anew for new bonding tasks. Therefore a model based investigation of the substructure vibration at various bond frequencies and its influence on the bond quality is presented. In addition to the model results, a series of tests using 300 μm copper wire and operating frequencies of 37, 60 and 100 kHz are utilized to identify the differences in the bond formation for a certain substrate. Key measurands are the wire

ISBN 978-3-8007-4540-1

deformation, velocity amplitudes of the tool tip and substructure as well as the shear force values over the bond duration. Digital microscopic pictures of the interface and the bonds are used to identify the welded areas in the interface and determine the width of the wire footprint.

2 Copper Wire Bonding Model

In the past, several approaches for modeling wire bonding have been reported. In [7] and [12], a friction based model approach for modeling the bond formation in the interface between wire and substrate was introduced. The bond process is activated due to frictional energy in the interface contact while the wire is excited by the tool tip, generating micro slip in the interface. Besides modeling the bond formation, in [3] and [8] a generalized model containing

- an electro-mechanical model of the ultrasonic transducer and the resonance controller,
- an ultrasonic softening model,
- and a reduced friction model based on [3]

was presented. Based on that generalized model, an extended model with substrate dynamics is presented here.

2.1 Generalized friction based modeling of bond formation

The differential equation system for modeling the bond formation is based on the two states γ and τ, **Eq. 1**. The first state γ represents the cleaning state of the interface and the second state τ the degree of weld strength, which can be related to the shear value. The friction power P_f leads to a rising cleaning state γ due to frictional wear of oxide layers in the contact. The cleaning state can have values from 0 up to 1. The weld strength is influenced by the cleaning state and the frictional power P_f; it is stated that remaining oxide layers aggravate the bond formation and an activation power P_0 is needed for a rising weld strength.

$$\begin{aligned} \dot{\gamma} &= \beta\, P_f && \forall \quad \gamma < 1 \\ \dot{\gamma} &= 0 && \forall \quad \gamma \geq 1 \\ \dot{\tau} &= \gamma\, \alpha\, P_f && \forall \; P_f \geq P_0 \\ \dot{\tau} &= 0 && \forall \; P_f < P_0 \end{aligned} \tag{1}$$

Both differential equations can be tuned by the coefficients β and α, which both have the unit $\frac{1}{J}$ while the states γ and τ are dimensionless. The values for the coefficients P_0, β and α are fitted to measurands.

2.2 Modeling substructure dynamics

For modeling the substructure dynamics, a modal description of elastic bodies is chosen. The modal description is beneficial in terms of reducing the number of degrees of freedom by approximating the dynamical behavior of the substructure with the most relevant modes while neglecting e.g. higher modes with less relevance on the dynamical behavior for the specific excitation. The theory is described

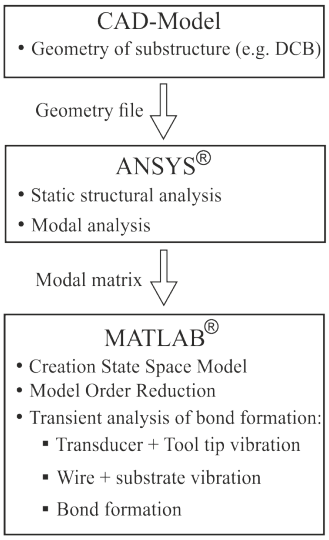

Figure 1 Workflow for creation of reduced state space model of the substructure dynamics, based on the numerical modal analysis in ANSYS.

in [9]; in the following the work flow for creating a dynamical model of flexible substructures is presented, **Figure 1**. In the first step, a CAD-model of the substructure is created. The geometry is imported into a finite elemente program (ANSYS) for a static structural analysis to simulate the static deformation of the substrate due to the bond normal force. The deformed geometry and its pre-stress are then used for a numerical modal analysis which generates a modal matrix. At this step, a wide frequency range is used to consider all relevant mode shapes. The modal matrix is then exported from ANSYS to MATLAB and a state space system is created. The created state space system has a high number of states because of the wide frequency range used. Thus, model order reduction (MOR) based on the Hankel Singular Values (HSV) is used. Small HSV identify states, that are neither controllable (the friction force is not able to excite the state/mode shape) nor observable (the state/mode shape has a small influence on the selected output). A more detailed insight on the theory of MOR and the creation of state space systems based on results of a numerical modal analysis is given in [10].

In the following a model based analysis of the system behavior at different working frequencies is carried out. As a substructure a DCB which is fixed on a rubber-plate is investigated and described in **Figure 2**.

As the bond position for the simulation, the edge of the top surface of the DCB was chosen; at this position different kinds of mode shapes with high relevance to the dynamical behavior of the substructure occur. The relevance can be judged by the described HSV. As a final step a reduced state space model is created and integrated in the generalized model of the bond process.

In the simulation two different working frequencies f_1 and f_2 are chosen; one smaller than the first resonance frequency of the substructure and one greater than the largest investigated resonance frequency of the substructure. The resulting frequency response of the tangential friction force

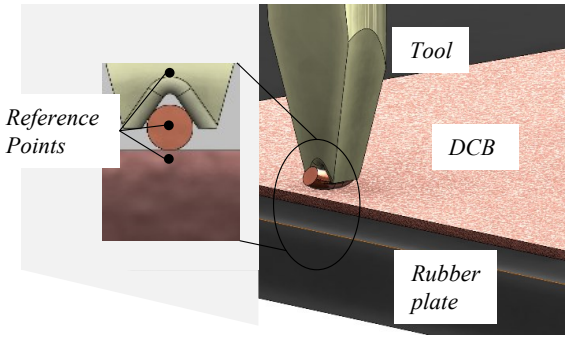

Figure 2 Model setup: the substructure consists of a DCB which is fixed to a rubber-plate. The model outputs are the amplitudes at the reference points on the end face of the tool, center of the wire and the edge of the DCB.

and the displacement amplitude at the reference point of the substructure is shown in **Figure 3**.

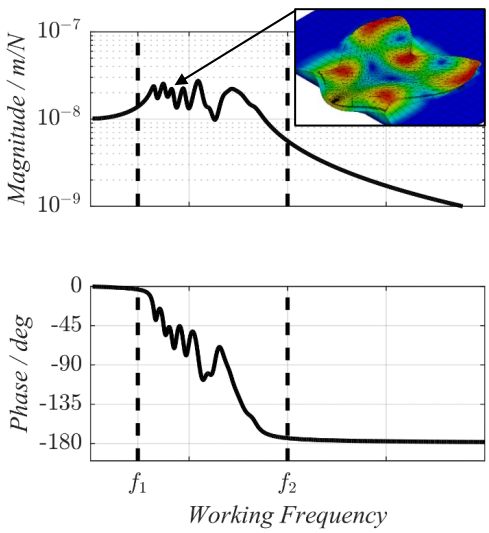

Figure 3 Frequency response of the substructure with the tangential friction force in the interface as an input and the displacement amplitude at the reference point of the substrate as an output. The third mode shape (in plane) of the substructure is exemplary shown.

2.3 Simulation Results

For the simulation, the parameters of the electromechanical model of the transducer are tuned to the desired working frequencies. The ultrasonic voltage is chosen such that the velocity amplitude at the tool tip is the same for both working frequencies in the unloaded case, oscillating freely. The bond duration was chosen in a way that the number of oscillations at the end of the bond process was the same for both working frequencies f_1 and f_2. The simulated velocity amplitudes of the wire and the substrate at the reference points, the weld strength τ and the phase differences of the movement between the tool and wire as well as between the wire and substrate are depicted in **Figure 4**.

Choosing the working frequency f_2, the wire overshoots

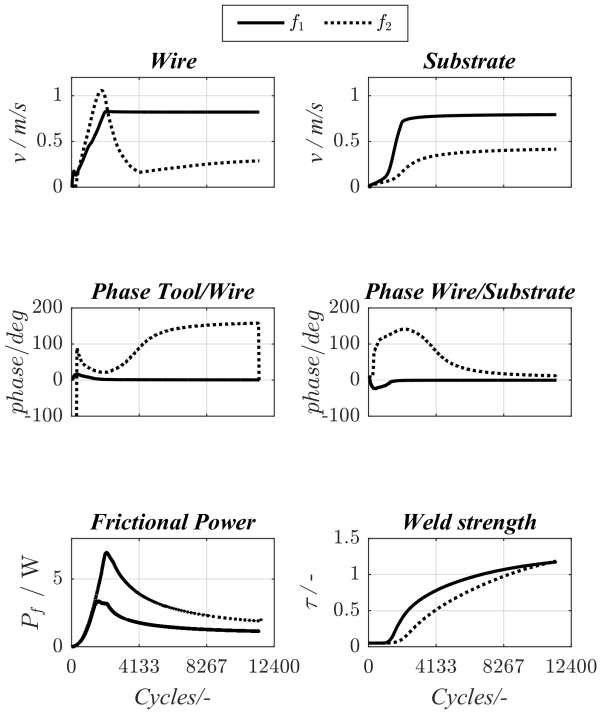

Figure 4 Simulation results: velocity amplitude of the wire and substrate, the phase difference between the tool and wire as well as between the wire and substrate, the frictional power in the interface and the weld strength τ.

in the cleaning phase at the beginning of the bond formation and then gets bonded to the substrate while the wire amplitude decreases. In comparison, the simulation results for the working frequency f_1 show a two times higher substrate amplitude and a different behavior of the wire movement; as the wire gets bonded to the substrate, the wire amplitude does not decrease significantly.

The dynamical behavior can be explained by the phase difference between the wire and substrate. In case of the working frequency f_1, the phase difference between wire and substrate is nearly zero; that means the wire moves in-phase with the substrate and the substrate adapts to the wire amplitude. That is in contrast to the working frequency f_2, where the wire first moves with 180° phase difference to the substrate and with rising bond formation it also adapts to the substrate vibration in a way that the phase difference decreases to nearly zero. When the wire is bonded to the substrate, the substrate amplitude rises significantly less compared to the frequency f_1. Due to the excitation with a frequency above the last relevant resonance frequency, the substructure acts like a dynamical absorber and thus the amplitude of the substrate is lower than in case of f_1. When the wire is bonded to the substrate, the slip between tool and wire rises, which can be seen in the rising phase between tool and wire.

As a result of the absorbing character of the substrate in case of the exciting frequency f_2 above the resonance frequency of the substructure, the frictional power is higher compared to f_1, even when the wire is bonded to the substrate. This leads to a different form of the welding curve τ with less saturation behavior.

3 Experiments

Based on the simulation results, two different experimental setups are examined more closely. In section 3.1, a principle experiment on a substructure with reduced geometrical complexity is used to validate the dynamical model behavior, **Figure 5**. The height h of the copper rod with a diameter of 1 mm can be varied to change the static stiffness as well as the resonance frequencies of the bending mode. For the experiment, two bond frequencies (37 kHz and 100 kHz) and two different heights (3.6 mm and 9.6 mm) of the copper rod are investigated. The height of the copper rod was determined to have a specific resonance frequency in relation to the bond frequency. Therefore, the resonance frequencies of both heights are measured by impulse excitation. The vibration amplitudes of the tool tip and substrate are measured by a laser vibrometer. All bonding experiments were performed using a Hesse Mechatronics BJ939 wire bonder, using different bondheads for different working frequencies.

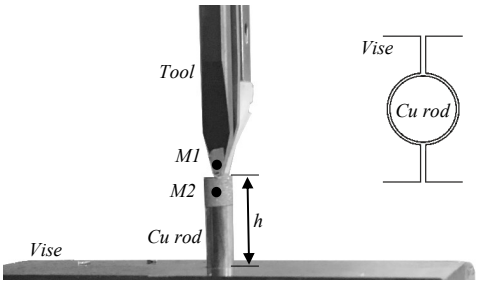

Figure 5 Setup of the prinicple experiment with a clamped copper rod in a modified vise. The height h can be varied and the velocity amplitudes at the positions M1 (tool tip) and M2 (edge of the copper rod) are measured.

The principle setup is not suitable for extensive experimental series because of the limited amount of wire bonds, that can be placed on one copper rod. Therefore, in section 3.2 a DCB which is fixed on a rubber-plate by a vacuum suction is used, to determine the shear force values, wire deformation and welded areas in the interface of pealed bonds. The wire deformation is directly captured by the bonding machine by recording the height of the tool position. Additionally the width of the foot prints is measured. Three bond frequencies (37 kHz, 60 kHz and 100 kHz) for bonding on the DCB substrate are used. For all three frequencies the same normal force was used. The voltage is adjusted, such that the velocity amplitude at the tool tip when being loaded with the bond normal force is the same for all three working frequencies. The bond duration is chosen, such that the number of oscillations at the end of the bond formation is the same for all three frequencies. The trajectories of the voltage over the bond time are shown in **Figure 6**.

3.1 Measuring the dynamical behavior of the substructure

The resonance frequencies of the copper rod at the two different heights are measured by impulse excitation. For the

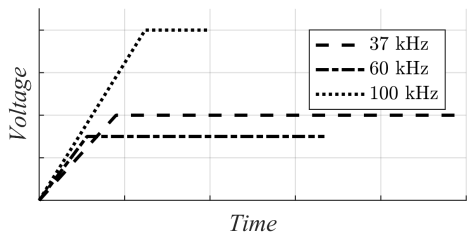

Figure 6 Trajectory of the voltage over the bond duration at the different working frequencies.

excitation, a spherical steel bullet with a diameter of 2 mm was rolled over a v-shaped slide against the top of the copper rod. The measured velocity response at the reference point M1 is then transformed into the frequency domain by the Fast Fourier Transform (FFT) of the transient velocity signal in MATLAB. The upper frequency limit for this method is dependent of the mass of the bullet and its stiffness; the method is described in [11].

The spectrum of the copper rod with a height of h=3.6 mm has two significant resonance frequencies at 45 kHz and 54 kHz that are identified as the first two bending modes of the copper rod, **Figure 7**. Two resonance frequencies of the first bending mode occur because of the anisotropic stiffness of the vise which clamps the rod. In this setup, the working frequency of 37 kHz can be linked to the frequency f_1 and the working frequency of 100 kHz to the frequency f_2 in the simulation.

The second setup (h=9.6 mm) shows the first bending modes at significantly lower frequencies (10 kHz and 11.5 kHz), additionally a torsion mode at 48 kHz, and the second bending modes at 56 kHz and 60 kHz occur. In this case, the working frequency 37 kHz as well as 100 kHz can be compared with f_2 of the simulation. The working frequency 37 kHz is greater than the resonance frequency of the first bending modes and the working frequency 100 kHz is greater than the resonance frequency of the second bending mode.

From the measurements with the laser vibrometer at the edge of the copper rod, it can be seen that in case of the working frequency 37 kHz and a height h=3.6 mm, significantly higher velocity amplitudes occur compared to the remaining three setups, **Figure 8**.

In this case, the phase difference between the tool and substrate is approximately 0° which corresponds to the simulation results for the working f_1; hence the higher substrate amplitudes can be explained with the forced inphase excitation of the substrate by the tool/wire vibration, **Figure 9**. When bonding with the same frequency of 37 kHz on the copper rod with the height of h=9.6 mm the substrate amplitude is decreased to approximately 10% of the amplitude at h=3.6 mm and the phase difference between tool and substrate movement reaches approximately 150°. In this case, the lower substrate amplitudes can be explained with the absorbing character of the copper rod with a height of 9.6 mm when being excited with 37 kHz, even though the static stiffness of the rod is lower compared to the rod with the height of 3.6 mm.

In case of the excitation frequency of 100 kHz, for both

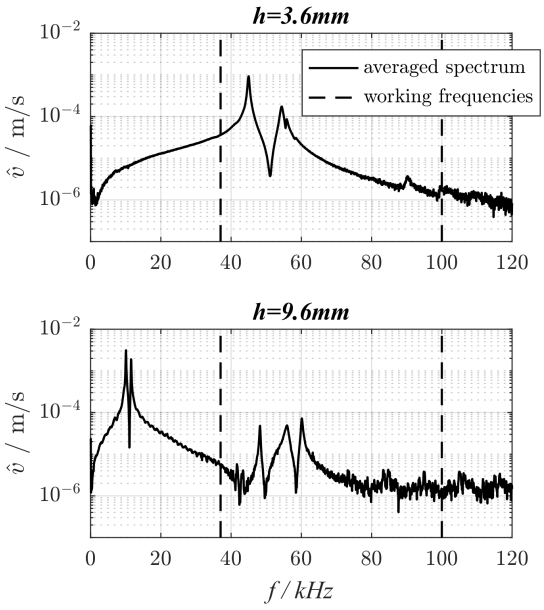

Figure 7 Resonance spectrum of principle setup with the height h=3.6 mm on the top and h=9.6 mm on the bottom. The averaged spectrum is based on five single measurements. The investigated working frequencies 37 kHz and 100 kHz are marked by the dashed lines.

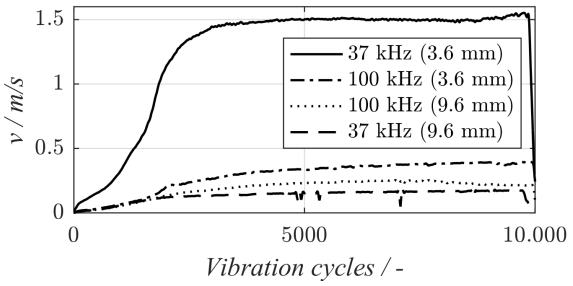

Figure 8 Velocity amplitude of the copper rod at the measurement position M2.

heights the working frequency lies above the relevant resonance frequencies of the substructure and in both cases, the substructure behaves like an absorber for the dynamical excitation.

3.2 Shear tests, wire deformation and image segmentation

For the three working frequencies 37 kHz, 60 kHz and 100 kHz the shear values and the wire deformation over the bond durations are measured at cutoff times with the same number of oscillation cycles for each frequency, **Figure 10**. For each cutoff time, 25 bonds were evaluated at the destination position. The trend of the deformation curves approximately follows the development of the shear values. For 100 kHz, the trend of the shear values and the deformation curve do not reach the saturation, while for 37 kHz and 60 kHz, the maximum of shear values and deformation is reached. The shear values at 10.000 oscillation cycles for 60 kHz and 100 kHz both reach approximately 32 N; for

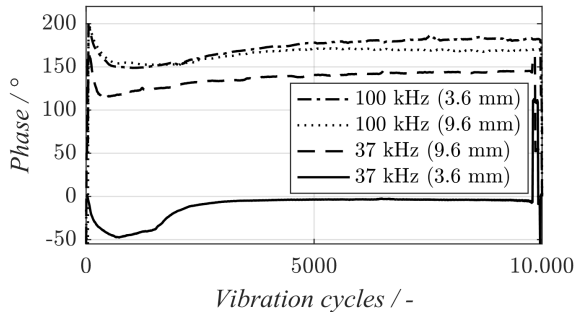

Figure 9 Phase difference between the tool tip movement and substructure movement at the measurement points M1 and M2.

37 kHz, the shear value reaches 27 N. The recorded wire deformation at the end of the bond process for the working frequency of 100 kHz is comparable to 37 kHz and larger than for 60 kHz.

In the experiments, the velocity amplitude at the tool tip for 37 kHz reached 1.2 $\frac{\mathrm{m}}{\mathrm{s}}$ and for 60 kHz and 100 kHz 1.4 $\frac{\mathrm{m}}{\mathrm{s}}$. Even though the voltage is chosen in a way that the velocity amplitude at the tool tip for all frequencies should achieve the same level, in case of 37 kHz a lower amplitude is observed which explains the lower shear value at the end of the bond formation. The behavior of the bond formation at 100 kHz matches with the simulation results at the frequency f_2; the trend of the welding curve in the simulation also does not show an early saturation behavior as with f_1. That is explained with the lower substrate amplitude and higher frictional power in the interface, even with the rising weld strength.

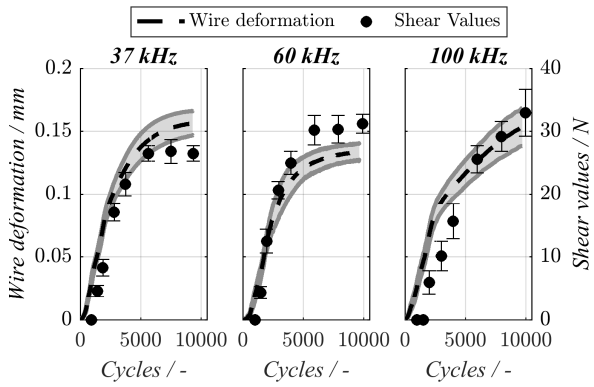

Figure 10 Shear values (mean and standard deviation values) at specific cutoff times with the same number of oscillations and measured wire deformation (mean value as dashed line and standard deviation as solid grey line).

The pictures of the pealed bond positions made using a digital microscope were analyzed by image segmentation [2], **Figure 11**. For 100 kHz the width of the elliptic interface is less compared to 37 kHz and 60 kHz. That corresponds to the measured width of the foot prints, **Table 1**. The distribution of the micro welds shows, that for 100 kHz a more homogenous welded area with an elliptic ring of high weld probability developed. For the working frequencies of 37

kHz and 60 kHz, the areas of high weld probability are aligned to the tool position and a less homogenous welded interface arises.

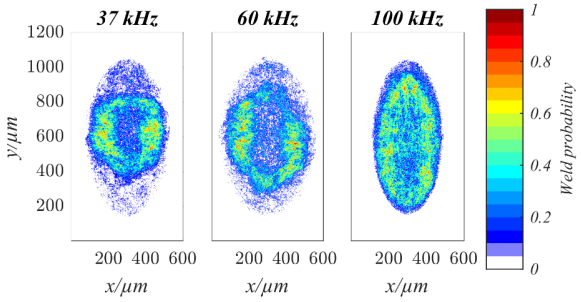

Figure 11 Results of image segmentation at 10.000 oscillation cycles of 15 pealed interface pictures at each frequency from digital microscopy.

Even though the recorded wire deformation at the bonding machine at 100 kHz was higher than at 60 kHz, it can be seen, that the deformation of the foot print was less compared to the lower frequencies. In further experiments, less susceptibility for heel cracks when pulling the bonds produced at 100 kHz was observed compared to the lower frequencies.

37 kHz	60 kHz	100 kHz
404 μm	391 μm	384 μm
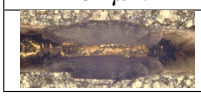	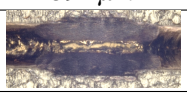	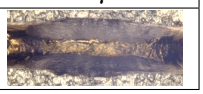

Table 1 Mean values (15 bonds) of the width of foot prints and representative pictures of the bonds.

4 Conclusion

Modeling the bonding process under consideration of substructure dynamics has led to a great increase in knowledge about the influence of working frequencies on the bond formation from a dynamical/mechanical point of view. The simulation and experimental results show, that bonding with a working frequency above a specific substructure resonance frequency leads to less substructure movement and thus to a more efficient usage of frictional power in the interface and less mechanical stress of the substructure. Thus the risk for failure modes like delamination of the DCB can be reduced while the bond strength remains the same or can even reach higher values due to a later saturation of the bond formation. Besides the shear values, also the bond deformation and the distribution of the welded areas in the interface have been measured. Bonding at a working frequency of 100 kHz achieves a more homogenous welded area in the interface and less width of the foot print compared to lower frequencies.
This may lead to new more detailed guide lines for the choice of the working frequency when bonding on challenging supple substrates. For the construction of semiconductor modules, the knowledge about the impact of the resonance frequencies of the substructure on the bond quality can be used for the design of the substructure stiffness at the bond position.

Acknowledgement

This research was supported by ERDF.NRW (European Regional Development Fund in North Rhine-Westphalia).

5 Literature

[1] D. Siepe, R. Bayerer, and R. Roth, “The future of wire bonding is? Wire bonding!,” Int. Conf. on Integrated Power Electronics Systems, 2010.

[2] A. Unger, R. Schemmel, T. Meyer, F. Eacock, P. Eichwald, S. Althoff, W. Sextro, M. Brökelmann, M. Hunstig and K. Guth, “Validated simulation of the ultrasonic wire bonding process,” IEEE CPMT Symposium Japan, 2016, pp. 251-254.

[3] T. Meyer, A. Unger, F. Eacock, P. Eichwald, S. Althoff, W. Sextro, M. Brökelmann, M. Hunstig and K. Guth, “Modeling and simulation of the ultrasonic wire bonding process,” 2015 17th Electronics Packaging Technology Conference, 2015.

[4] J.L. Harthoorn, “Ultrasonic metal welding,”PhD thesis, Eindhoven University, pp. 89-97, 1978.

[5] J.K. Kim and Y.M. Cheung, “Effects of bonding frequency on Au wedge wire bondability,” Journal of Materials Science: Materials in Electronics, March 2008.

[6] L. Levine, “The ultrasonic wedge bonding mechanism: two theories converge,” Proc. SPIE— Int. Soc. Opt. Eng., vol. 2649, pp. 242-246, 1995.

[7] S. Althoff, J. Neuhaus, T. Hemsel and W. Sextro, “A friction based model approach for modeling wire bonding,” IMAPS 2013, 46th International Symposium on Microelectronics, 2013.

[8] A. Unger, W. Sextro, T. Meyer, P. Eichwald, S. Althoff, F. Eacock, M. Brökelmann, M. Hunstig and K. Guth,“ Modeling of the stick-slip effect in heavy copper wire bonding to determine and reduce tool wear,” 2015 17th Electronics Packaging Technology Conference, 2015.

[9] W. Sextro, “Dynamical contact problems with friction, models, methods, experiments and applications,” Springer Vieweg Verlag, 2007.

[10] M.R. Hatch, “Vibration Simulation Using MATLAB and ANSYS,”Chapman & Hall/CRC, 2001.

[11] J. Rosseels, “Resonant piezoelectric motors - Impact of mechanical machining deviations and methods to cope with them,” PhD thesis, KU Leuven University, pp. 45-59, 2016.

[12] H. Gaul, “Berechnung der Verbindungsqualität beim Ultraschall-Wedge/Wedge-Bonden,” PhD thesis, Berlin, Technical University, 2009.

